Translational Oncology
www.transonc.com

Volume 1 Number 2 July 2008 pp. 95–101 95

Molecular Characterization of Synovial Sarcoma in Children and Adolescents: Evidence of Akt Activation[1]

Fabio Bozzi*, Andrea Ferrari†, Tiziana Negri*, Elena Conca*, Da Riva Luca*, Marco Losa*, Paola Casieri*, Marta Orsenigo*, Andrea Lampis*, Cristina Meazza†, Michela Casanova†, Marco A. Pierotti‡, Elena Tamborini* and Silvana Pilotti*

*Experimental Molecular Pathology, Department of Pathology, Istituto Nazionale Tumori, Milan, Italy; †Department of Medical Oncology, Division of Pediatrics

Abstract

Synovial sarcoma (SS) is the most frequent nonrhabdomyosarcomatous soft tissue sarcoma encountered in adolescents and young adults, and despite advances in the treatment of local disease, metastases remain the main cause of death. The aim of this study was to characterize a single-center series of pediatric SS molecularly to seek any biomarkers or pathways that might make suitable targets for new agents. Seventeen cases of pediatric SS showing the *SYT–SSX* fusion transcript were screened immunohistochemically, biochemically, molecularly, and cytogenetically (depending on the available material) to investigate any expression/activation of epidermal growth factor receptor, platelet-derived growth factor receptor alpha (PDGFRα), PDGFRβ, Akt, and deregulated Wnt pathway. The most relevant outcome was the finding of activated epidermal growth factor receptor, PDGFRα, and PDGFRβ, which activated Akt in both the monophasic and biphasic histologic subtypes. Consistently, Akt activation was completely abolished in an SS cell line assay when stimulated by PDGF-AA and treated with the phosphatidylinositol 3-kinase inhibitor LY294002. Our results also showed the nuclear localization of β-catenin and cyclin D1 gene products in monophasic SS and the movement of β-catenin into the cytoplasm in the glandular component of the biphasic subtype. Although they need to be confirmed in larger series, these preliminary data suggest that therapeutic strategies including specific inhibitors of the phosphatidylinositol 3-kinase/Akt pathway might be exploited in SS.

Translational Oncology (2008) 1, 95–101

Introduction

Synovial sarcoma (SS) is one of the most common mesenchymal malignancies and accounts for approximately 8% to 10% of all soft tissue sarcomas; it is also reported to be the most frequent nonrhabdomyosarcomatous soft tissue sarcoma encountered in adolescents and young adults (15–20% of cases). It is characterized by the specific chromosomal translocation t(X;18) (p11;q11) that fuses the *SYT* gene from chromosome 18 with the *SSX1* (approximately 2/3 of cases), *SSX2* (approximately 1/3 of cases), or *SSX4* gene (rare cases) from the X chromosome. Although it is thought that *SYT–SSX* plays a central part in the development of SS, the mechanism of tumor initiation is still unknown.

Gene array and immunohistochemistry (IHC) studies have recently identified high epidermal growth factor receptor (*EGFR*), *Her-2/neu*, *IGF2* and *HGFR* gene expression in SS [1,2], but the correlation between this and the activation of specific cascades [such as phosphatidylinositol 3-kinase (PI3K)/Akt] has not been fully investigated.

Akt is an intracellular serine/threonine kinase, which, once activated by PI3K, moves from the cell membrane to the cytoplasm and/or nucleus, where it controls survival (by inhibiting pro- and activating

Address all correspondence to: Silvana Pilotti, Unit of Experimental Molecular Pathology, Department of Pathology, Istituto Nazionale per lo Studio e la Cura dei Tumori, Via G. Venezian 1, 20133 Milano, Italy. E-mail: silvana.pilotti@istitutotumori.mi.it

[1]Supported by grants from Associazione Italiana per la Ricerca sul Cancro to S.P.
Received 15 May 2008; Revised 27 May 2008; Accepted 29 May 2008

1522-8002/08/$25.00 DOI 10.1593/tlo.08121

antiapoptotic factors), proliferation (by means of direct p21 and p27 phosphorylation), and other activities essential to tumor progression, such as angiogenesis, invasion, and metastasis. It is a key activator of the mammalian target of rapamycin that induces the expression of proangiogenic genes by stabilizing the hypoxia-inducible factor. In addition to direct GSK3B inactivation, it has also been shown that Akt directly phosphorylates the β-catenin Ser 552 residue in epithelial cancer cells [3] leading to the nuclear shift/activation of β-catenin.

In cell adhesion and transcription functions, β-catenin has the appropriate selection of which is crucial for normal development and the avoidance of cancer. It is well known that there is a striking cytoplasmic and nuclear accumulation of β-catenin in most SS, which is consistent with the recently reported presence of a transcriptionally active nuclear complex containing *SYT–SSX2* and β-catenin [4] and supports the idea that the sarcoma chimeric protein contributes to cancer formation by activating one of the β-catenin–targeted programs. However, because the accumulation of β-catenin in SS does not apparently depend on canonical Wnt activation and mutations in APC, β-catenin, and E-cadherin are rare [5,6], it may be that β-catenin is stabilized through its phosphorylation by receptor tyrosine kinases (RTKs) [7].

Bearing this in mind, after making a preliminary immunophenotypic analysis, we investigated 17 cases of pediatric SS—all with an *SYT–SSX* fusion transcript—using molecular biochemical methods suited to the type of material available (formalin-fixed or frozen) to seek any potential biomarkers or pathways that might be suitable targets for licensed drugs, such as the expression of EGFR, platelet-derived growth factor receptor alpha (PDGFRα), PDGFRβ, Akt, and deregulated Wnt pathways.

Our findings support the expression and activation of EGFR, PDGFRα, and PDGFRβ, which may activate Akt. These albeit preliminary data suggest that therapeutic strategies including specific inhibitors of the PI3K/Akt pathway might be exploited in SS.

Materials and Methods

Patients and Materials

We analyzed specimens from 17 patients with SS (nine males and eight females aged 7–18 years; median age, 11 years), all but one of whom (BSS8 in Table 1) were treated at the Pediatric Oncology Unit of the Fondazione IRCCS, Istituto Nazionale Tumori, Milan, Italy. All of the specimens came from primary tumors and had been obtained before any treatment had been given, and representative samples obtained from formalin-fixed material were immunophenotyped. All of the biochemical and molecular analyses were made using frozen sections after the tumoral component had been carefully dissected under a microscope to avoid contamination by normal or necrotic tissue.

Written informed consent was obtained from all of the patients and/or their parents or legal guardians.

Immunohistochemistry

The samples were immunophenotyped using the following antibodies and dilutions: PDGFRα (C-20), sc-338 rabbit polyclonal IgG (Santa Cruz Biotechnology Inc., Santa Cruz, CA) diluted 1:200; PDGFRβ (P-20), sc-339 rabbit polyclonal IgG (Santa Cruz Biotechnology) diluted 1:100; KIT, rabbit polyclonal antihuman CD117 (code A 4502; Dako, Carpinteria, CA) diluted 1:50; HER2/NEU, c-erb-2 rabbit polyclonal antihuman Oncoprotein (code A 0485; Dako) diluted 1:2000; cyclin D1 rabbit monoclonal antibody clone SP4 (code RM-9104-S1; Lab Vision, Fremont, CA) diluted 1:100; β-catenin mouse monoclonal antibody (clone 14, code C19220; Transduction Laboratories, Lexington, KY) diluted 1:2000.

The antigens for all antibodies were retrieved using 5 mM citrate buffer (pH 6) in an autoclave at 95°C for 6 minutes, except for cyclin D1 and β-catenin, which took 30 minutes. All of these antibodies were developed as described elsewhere [8].

Epidermal growth factor receptor was immunostained using the EGFR-pharmDx kit (code K1492; Dako) following the manufacturer's instructions. The EGFR-immunostained cells were quantitatively evaluated, and their staining intensity was scored as described elsewhere [9]. The following positive controls were used in each IHC experiment: one case of fibromatosis for PDGFRα and PDGFRβ, one case of KIT-mutated GIST for KIT, one case of ductal salivary gland carcinoma for HER2/NEU, one case of colon carcinoma for β-catenin, and one case of mantle cell lymphoma for BCL1.

Table 1. Clinical Characteristic of Pediatric SS Patients.

	Age (years)	Site	Stage	Therapy	Relapse	Status
MSS1	17	Lower extremity	T2 B N0 M0	S + CT + RXT	74 months	DOD (106 months)
MSS2	7	Lower extremity	T2 B N0 M0	S + CT + RXT	68 months	DOD (120 months)
MSS3	16	Lower extremity	T2 B N0 M0	S + CT + RXT	32 months	PRO (150 months)
MSS4	17	Lower extremity	T1 B N0 M0	S + CT + RXT	No	First CR (140 months)
MSS5	17	Pleura	T2 B N0 M0	S + CT + RXT	9 months	DOD (14 months)
MSS6	11	Upper extremity	T1 A N0 M0	S + CT + RXT	No	First CR (102 months)
MSS7	10	Lower extremity	T2 B N0 M0	S + CT + RXT	50 months	DOD (58 months)
MSS8	15	Lower extremity	T2 A N0 M0	S + CT + RXT	No	First CR (140 months)
BSS1	15	Lung	T2 B N0 M0	S + CT + RXT	18 months	DOD (50 months)
BSS2	10	Upper extremity	T1 A N0 M0	S + CT	No	First CR (88 months)
BSS3	18	Head/neck	T2 B N0 M0	S + CT + RXT	No	First CR (62 months)
BSS4	10	Lower extremity	T2 B N0 M0	S + CT + RXT	56 months	Third CR (170 months)
BSS5	15	Lower extremity	T2 B N0 M0	S + CT	8 months	DOD (72 months)
BSS6	12	Abdominal wall	T2 B N0 M0	S + CT	No	First CR (125 months)
BSS7	15	Lower extremity	T2 B N0 M0	S + CT + RXT	No	First CR (36 months)
BSS8	14	Lower extremity	NA	NA	NA	NA
BSS9	12	Lower extremity	T2 A N0 M0	S + CT + RXT	No	First CR (200 months)

TNM classification based on local invasiveness, T1 and T2, and tumor size, A or B, i.e., less or more than 5 cm; absence or presence of nodal and distant involvement: N0 and N1, M0 and M1, respectively [Harmer MH (1982). *TNM Classification of Pediatric Tumors*. UICC International Union Against Cancer, Geneva, Switzerland. pp. 23–28].
CR indicates complete remission; *CT*, chemotherapy; *DOD*, dead of disease; *NA*, not available; *PRO*, progressive disease; *RXT*, radiotherapy; *S*, surgery.

Biochemical Analysis

Protein extraction and immunoprecipitation/Western blot analysis. The EGFR, PDGFRα, and PDGFRβ proteins were extracted, immunoprecipitated, and blotted as described elsewhere [8]. The A431 cell line (American Type Culture Collection, Manassas, VA) was used as a positive control for the EGFR protein expression/phosphorylation experiments, and the NIH3T3 cell line (American Type Culture Collection) for the PDGFRα protein expression/phosphorylation experiments.

Twenty micrograms of cytoplasmic total protein extract was used with anti–phospho-Akt Ser 473 polyclonal antibody (#9271; Cell Signaling Technology, Beverly, MA) diluted 1:1000 in the Akt Western blot (WB) experiments, and the filters were subsequently stripped and incubated with anti-Akt polyclonal antibody (#9272; Cell Signaling) diluted 1:1000; the NIH3T3 cell line was used as a positive control. Thirty micrograms cytoplasmic total protein extract was used with the anti–phospho-β-catenin Y142 (clone ab27798; Abcam, Cambridge, UK) diluted 1:1000 in the β-catenin WB experiments, and the filters were subsequently stripped and incubated with anti—β-catenin (clone BDI109; Abcam) diluted 1:1000; the A431 cell line was used as a positive control.

CME-1 Cell Line Culture Conditions

The CME-1 cell line was cultured as previously described [10]. For the biochemical analyses, the CME-1 cells were serum-starved for 16 hours, and then stimulated with 50 ng/ml of PDGF-AA (catalogue 100-13A; PeproTech, Princeton, NJ) for 5, 15, 30, and 60 minutes. The PI3K inhibitor LY294002 (kindly provided by Dr. L. Lanzi, Experimental Oncology Unit, Fondazione IRCCS, Istituto Nazionale Tumori, Milan, Italy) was used at volumes of 0.5, 5, and 50 μM in CME-1 serum-starved cells stimulated with 50 ng/ml of PDGF-AA for 15 minutes.

The WB analyses were made as described above for the primary specimens.

RNA Extraction, Reverse Transcription, and cDNA Synthesis

Total RNA was extracted from formalin-fixed materials and reverse-transcribed. All of the samples were tested for cDNA integrity and DNA contamination by amplifying the *β-actin* and *HPRT* (hypoxanthine guanine phosphoribosyl transferase) housekeeping genes.

Detection of Fusion Transcripts by Polymerase Chain Reaction and Fluorescence In Situ *Hybridization*

SYT/SSX fusion transcripts were detected by polymerase chain reaction (PCR) as described in detail elsewhere [11]. Briefly, good-quality RNA was obtained from all 17 samples, all of which showed the *SYT–SSX* gene fusion transcript: 11 (65%: 5/8 monophasic cases and 6/9 biphasic cases) carried *SYT–SSX1* and six (35%: 3/8 monophasic and 3/9 biphasic cases) carried *SYT–SSX2* (Table 2).

In all cases, the presence of an *SYT–SSX* translocation was confirmed by fluorescence *in situ* hybridization (FISH) analysis using BAC probes RP11-38O23 and RP11-344N17 for *SSX1*, RP11-552J9 and RP13-77O11 for *SSX2*, and RP11-737G21, RP11-786F14, and RP11-399L5 for *SYT* as previously described [12].

EGFR and PDGFRα FISH Analyses

These were made using previously described probes [8].

Relative Quantification of RTK Receptor and Ligand Expression

Epidermal growth factor receptor, PDGFRα, PDGFRβ, PDGFA, TGFA, and glyceraldehyde-3-phosphate dehydrogenase cDNAs were relatively quantified by means of real-time quantitative PCR (ABI PRISM 5700 PCR Sequence Detection Systems; Applied Biosystems, Foster City, CA) using a *Taq*Man-based analysis and following the

Table 2. Immunostaining Results of Pediatric SS Patients.

	Syt/ssx		β-Catenin	BCL1	EGFR	HER2/NEU	PDGFRα	PDGFRβ	KIT
MSS1	2		++N	+N	4 + 3 high	–	+/–	+	–
MSS2	1		++N	+N	3 + 3 high	–	++	+	–
MSS3	2		++N	+N	3 + 2 high	–	++	+/–	–
MSS4	1		++N	+N	2 + 2	–	++	+	–
MSS5	2		++N/C	+N	2 + 2	–	++	+	–
MSS6	1		++N/C	+N	4 + 3 high	–	++	+/–	–
MSS7	1		++C	+N	4 + 3 high	–	+/–	+	–
MSS8	1		+C/N	+N	2 + 2	–	+	+	–
BSS1	1	Gland comp.	+ C/M	++N	—	–	++	+/–	–
		Spindle comp.	—	—	High	–	++	+/–	–
BSS2	1	Gland comp.	+ C/M	++N	—	–	++	+/–	+/–
		Spindle comp.	—	—	High	–	++	+/–	–
BSS3	1	Gland comp.	+ C/M	++N	—	–	++	+/–	+/–
		Spindle comp.	—	—	High	–	++	+/–	–
BSS4	1	Gland comp.	+ C/M	++N	—	+/–	++	+	+/–
		Spindle comp.	—	—	High	–	++	+	–
BSS5	1	Gland comp.	+ C/M	++N	—	–	++	+	–
		Spindle comp.	—	—	High	–	+/–	+	–
BSS6	2	Gland comp.	+ C/M	++N	—	+/–	+/–	+/–	+/–
		Spindle comp.	—	—	High	–	++	+/–	+/–
BSS7	1	Gland comp.	+ C/M	++N	—	+/–	++	+/–	+/–
		Spindle comp.	—	—	High	–	++	+/–	+/–
BSS8	2	Gland comp.	+ C/M	++N	—	–	++	+/–	–
		Spindle comp.	—	—	High	–	++	+/–	–
BSS9	2	NV	NV	NV	NV	NV	NV	NV	NV

– indicates no immunoreactivity; +/–, mild immunoreactivity; +, moderate immunoreactivity; ++, strong immunoreactivity; *BSS*, biphasic synovial sarcoma; *C*, cytoplasmatic staining; *Gland comp.*, glandular component; *M*, membrane staining; *MSS*, monophasic synovial sarcoma; *N*, nuclear staining; *NV*, not valuable; *Spindle comp.*, spindle component.

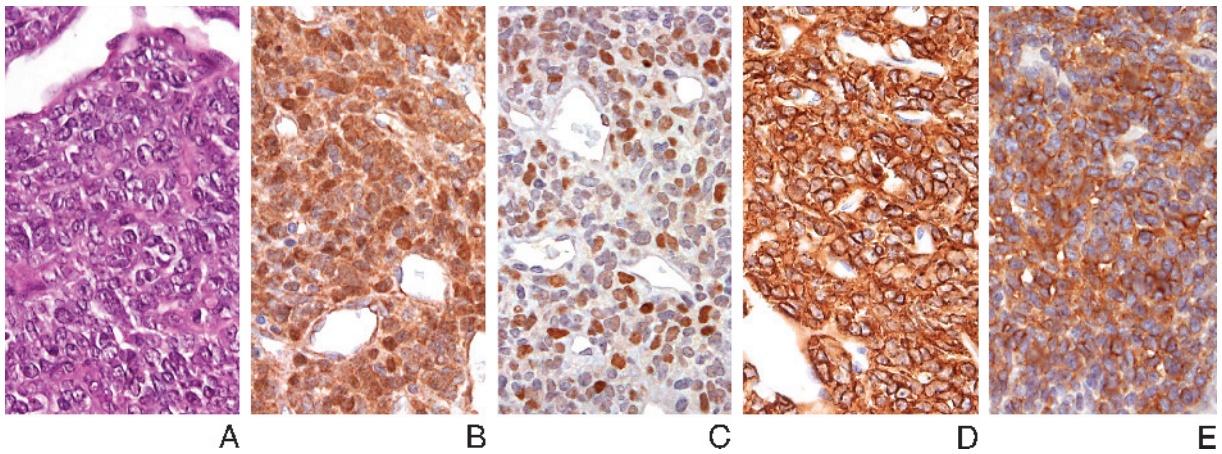

Figure 1. H/E section (A) of MSS3 (Table 1) showing β-catenin (B) and bcl1 (C) nuclear immunostaining, EGFR cytoplasmic membrane overexpression (D), and PDGFRα cytoplasmic decoration (E).

manufacturer's instructions. The relative changes in gene expression were calculated using the $2^{-\Delta\Delta C_t}$ method [13].

APC and β-Catenin Mutations

DNA was extracted from selected paraffin-embedded sections of six MSS showing nuclear β-catenin, and β-catenin exon 3 was amplified as previously described [14]. No activating mutations were found in these samples.

Results

Immunohistochemistry

Immunostaining was successful in all but case BSS9. The results are shown in Table 2 and Figures 1 and 2 (MSS3 and BSS4, respectively).

Receptor tyrosine kinases: EGFR, PDGFRα, PDGFRβ, KIT, and HER2/NEU. Epidermal growth factor receptor immunoreactivity was high [9] in the cytoplasm of almost all of the tumor cells in five of eight MSS but was restricted to the spindle cell component in all of the BSS samples. Her2/Neu was negative in all of the MSS but showed mild cytoplasmic reactivity in the glandular component of three of nine BSS. Platelet-derived growth factor receptor α was reactive in the cytoplasm of most of the MSS tumor cells and in the spindle and glandular cells of the BSS; the same was true of PDGFRβ, but the intensity of the staining was less in half the cases.

There was no Kit decoration in any of the MSS, and it was restricted to the cytoplasm of the glandular component in five of nine BSS, as previous reported [15].

β-Catenin and cyclin D1 products (bcl1). Because cyclin D1 can be considered a marker of β-catenin activation, we evaluated the immunoreactivitiy of both proteins.

Most tumor cells in six of eight MSS cases showed nuclear or nuclear/cytoplasmic β-catenin immunoreactivity, whereas cytoplasmic and cell membrane immunostaining was restricted to the glandular component in all of the BSS.

Nuclear bcl1 immunoreactivity was observed in 50% to 80% of the MSS tumor cells and decorated all of the nuclei of the glandular component in the BSS.

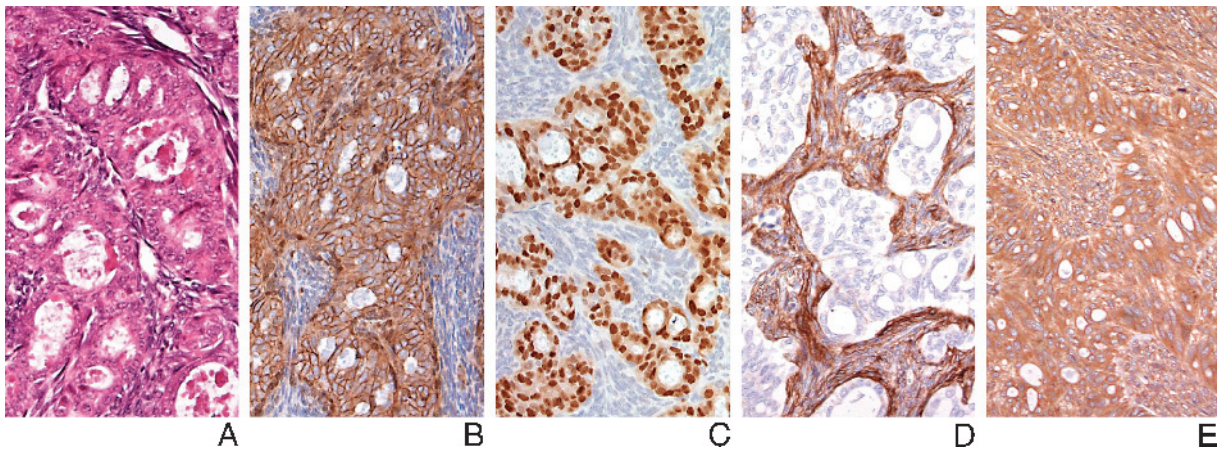

Figure 2. Hematoxylin and eosin–stained section (A) of BSS4 (Table 1) showing β-catenin expression and bcl1 restricted to the glandular component (B and C); β-catenin has a cytoplasmic membrane staining pattern (B) and bcl1 decorates the nuclei (C). Conversely, EGFR expression highlights the spindle cell tumor component (D). Platelet-derived growth factor receptor α cytoplasmic immunostaining is shared by both the epithelial and the spindle cell component (E).

Relative Quantification of PDGFRα, PDGFRβ, and EGFR mRNA Expression

Using a pool of normal mesenchymal-derived tissues as calibrators, we observed an increase in the transcripts of EGFR (median, 1.7×10^1; range, 1×10^0 to 1.9×10^2) and PDGFRα (median, 5×10^0; range, 1×10^0 to 6.4×10^1); the median level of the PDGFRβ transcript was similar to that of the calibrator (median, 1×10^0; range, 1×10^{-1} to 4×10^0). These results support the high IHC EGFR and PDGFRα scores in both the MSS and BSS.

Detection of EGFR and PDGFRα Ligands

Real-time PCR revealed the presence of the cognate ligand of PDGFRα (PDGF-AA) and EGFR (TGFA) in all cases. Given the lack of appropriate calibrators for the relative quantification of PDGF-AA and TGFA, we compared their median C_t values (26.5; range, 21.9–29.7 for PDGF-AA; and 31.2; range, 27.3–34.8 for TGFA) with that of the *Gapdh* housekeeping gene (25.9; range, 21.1–29).

Receptor Tyrosine Kinase Biochemical Analysis: EGFR, PDGFRα, and PDGFRβ Expression and Phosphorylation

Because the IHC results suggested that the RTKs expressed in most of the SS samples were EGFR, PDGFRα and, to a lesser extent, PDGFRβ, we investigated their activation in immunoprecipitation (IP)/WB analysis experiments.

Frozen samples of four MSS (#3, #4, #5, and #8) and three BSS (#1, #4, and #8) were available for biochemical analysis (frozen sections from both BSS1 and BSS4 had revealed an extensive glandular component on histologic examination). After specific IP (with anti-EGFR, anti-PDGFRα, and anti-PDGFRβ) and WB, all of the samples expressed activated (i.e., phosphorylated) EGFR (Figure 3*A* and Table 3), PDGFRα (Figure 3*B* and Table 3), and PDGFRβ (not shown).

AKT Phosphorylation

To confirm RTK activation further, we investigated the presence and activation of the shared downstream effector Akt, the phosphorylation of which was evaluated directly by means of WB. This experiment revealed phosphorylated Akt in six of seven SS samples (Figure 3*C* and Table 3).

Specific Inhibition of PI3K Abolishes PDGF-AA–Induced Akt Phosphorylation in the CME-1 SS Cell Line

Time-course studies of Akt activation (in the form of the phosphorylation of Akt Ser 473 in response to PDGF-AA stimulation) showed Akt activation in serum-starved CME-1 cells as early as 5 minutes after stimulation with 50 ng/ml PDGF-AA; this peaked after 15 minutes and returned to baseline values after 1 hour (not shown).

We next examined the effects of the established PI3K inhibitor LY294002 on Akt activation in serum-starved and LY294002-treated

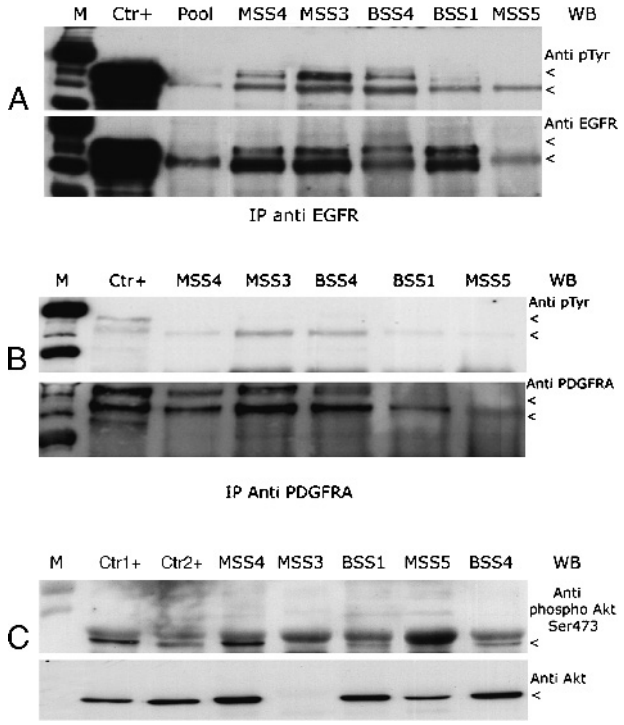

Figure 3. EGFR, PDGFRα, and Akt expression and activation in pediatric SS. (A) EGFR expression and activation. *Ctr+* indicates the A431 cell line used as a positive control; *M*, marker; *Pool*, protein pool derived from healthy mesodermal tissues; *MSS3*, *MSS4*, *MSS5*, *BSS1*, and *BSS4*, proteins extracted from frozen SS samples. The receptor was represented by two bands (depending on its glycosylation status) and is indicated by two arrows. (B) PDGFRα expression and activation. *Ctr+* indicates the NIH3T3 cell line used as a positive control; *M*, marker; *MSS3*, *MSS4*, *MSS5*, *BSS1*, and *BSS4*, proteins extracted from frozen SS samples. The receptor is indicated by two arrows. (C) Akt expression and activation. *Ctr1+* indicates the NIH3T3 cell line treated with PDGF as a positive control for Akt phosphorylation; *Ctr2+*, untreated NIH3T3; *M*, marker (93.6 and 106.9 kDa); *MSS3*, *MSS4*, *MSS5*, *BSS1*, and *BSS4*, proteins extracted from frozen SS samples. The arrow indicates that the pAKT is the lower band.

Table 3. Results of Biochemical Analysis of Frozen SS Samples.

	Akt		β-Catenin		EGFR		PDGFRα		PDGFRβ	
	Protein	pSer473	Protein	pTyr142	Protein	Phospo.	Protein	Phospo.	Protein	Phospo.
MSS3	+/–	–	+	+	+	+	+	+	+	+
MSS4	+	+	Nd	Nd	+	+	+	+	+	+
MSS5	+	+	–	–	+	+	+	+	+	+
MSS8	+	+	+	+	+	+	+	+	+	+
BSS1	+	+	+	+	+	+	+	+	+	+
BSS4	+	+	+	+	+	+	+	+	+	+
BSS8	+	+	+	–	+	+	+	+	+	+

BSS indicates biphasic synovial sarcoma; *MSS*, monophasic synovial sarcoma; *Nd*, not done; *phospho.*, phosphorylation detected by anti–pTYR after specific IP; *pSer473*, phosphorylation status of Ser 473 detected directly by WB; *pTyr142*, phosphorylation status Tyr 142 detected directly by WB.

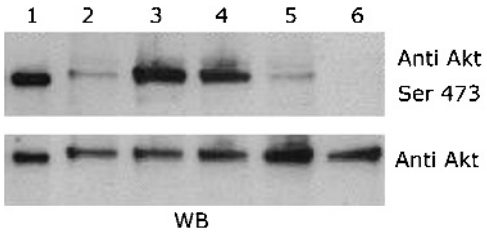

Figure 4. Akt activation and inhibition in the CME-1 SS cell line. The NIH3T3 cell line (lane 1) was used as a positive control. The cell showed low Akt phosphorylation after starvation (lane 2), but a high degree of activation when it was stimulated with 50 ng/ml of PDGF-AA for 15 minutes (lane 3). Akt Ser 473 phosphorylation was progressively reduced when the LY294002 PI3K inhibitor was added at 0.5, 5, and 50 μM (lanes 4, 5, and 6).

CME-1 cells and observed that Akt Ser 473 phosphorylation was completely abolished by the addition of 50 μg/ml LY294002 (Figure 4).

Receptor Tyrosine Kinase FISH Analysis

Because gene amplification is one of the mechanisms responsible for RTK activation, we investigated EGFR, PDGFRα, and PDGFRβ gene copy numbers by means of FISH in two MSS (#1 and #6) and three BSS (#3, #5, and #7), all of which showed a normal disomic hybridization pattern for all RTK receptors, which is consistent with the absence of gene amplification.

Receptor Tyrosine Kinases and β-Catenin

As a further step, we extracted cytoplasmic β-catenin and assessed its phosphorylation in tyrosine 142 (Y142). Western blot analysis showed that all of the tested BSS samples (BSS1, BSS4, and BSS8) had cytoplasmic β-catenin (thus confirming the IHC results), and β-catenin Y142 phosphorylation was observed in BSS1 and BSS4 (Figure 5 and Table 3). Despite the definite prevalence of nuclear β-catenin as IHC decoration in our MSS samples, Y142-phosphorylated cytoplasmic β-catenin was also observed by WB in MSS3 and MSS8 (Figure 5 and Table 3), thus suggesting that IHC is not sensitive enough to indicate β-catenin localization precisely.

In light of the above data, it can be assumed that the cytoplasmic localization of β-catenin very often parallels its phosphorylation in Y142. Because β-catenin Y142 phosphorylation can be achieved by means of the formation of β-catenin/RTK complexes or the activation of RTKs, and our IHC and IP/WB results suggested EGFR and PDGFRα activation, the filters obtained after IP/WB analysis with anti-EGFR and anti-PDGFRα were stripped and incubated with the anti–β-catenin antibody. No β-catenin/EGFR or β-catenin/PDGFRα coimmunoprecipitation was observed in either the MSS or the BSS specimens (not shown).

Discussion

The most relevant finding of this comprehensive investigation of a small, single-center series of pediatric SS cases is the presence of activated (i.e., phosphorylated) EGFR, PDGFRα, and Akt, which was supported by the biochemical results on snap-frozen material; we have previously reported the activation of PDGFRβ in a series of cryopreserved SS specimens taken from adults [11]. It is also worth noting the IHC evidence of nuclear β-catenin expression coupled with a cyclin D1 product (bcl1) in paraffin-embedded tissue; as previously reported [16,17], these results confirm that cyclin D1 can be considered one of the targets of activated β-catenin in SS.

Our biochemical data relating to cryopreserved samples and IHC data relating to formalin-fixed material (all showing overexpressed and activated EGFR, PDGFRα, and PDGFRβ), together with the demonstration of each receptor's cognate ligand by real-time PCR, support the idea that Akt is activated in response to multiple signals acting through the receptors through an autocrine/paracrine–mediated loop. This was confirmed by the absence of the activating mutation in EGFR [18] or PDGFRα [19] and the fact that the FISH data ruled out any gene alteration in the involved RTKs. In line with these findings, the Akt activation induced by PDGF-AA in the CME-1 SS cell line was completely abolished by the specific PI3K inhibitor LY294002, thus confirming that the PI3K/Akt pathway is biologically active in SS cell lines and is a potential therapeutic target in SS patients.

We also found a nuclear β-catenin expression in MSS and the increased expression of cyclin D1 (a β-catenin target gene) in both MSS and BSS. These findings not only indicate that this gene is activated but also suggest a possible mechanism underlying the β-catenin activation. The absence of *β-catenin* gene mutations in the six MSS showing nuclear β-catenin immunoreactivity and the absence of RTK/β-catenin complexes at IP analysis rule out the possibility that either are responsible for the nuclear localization of β-catenin; however, because our model highlighted the presence of activated Akt (a serine/threonine kinase downstream target of EGFR, PDGFRα, and PDGFRβ), this could presumably assist the nuclear translocation of β-catenin through its serine 552 phosphorylation or the direct inhibition of GSK3B [3]. Unfortunately, the lack of protein extract from

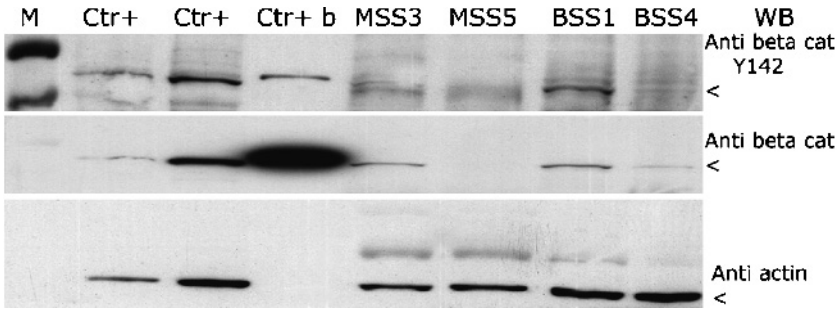

Figure 5. β-Catenin expression and activation. *Ctr+* indicates the A431 cell line used as a positive control; *Ctr+b*, bacterial recombinant β-catenin; *M*, marker; *MSS3*, *MSS5*, *BSS1*, and *BSS4*, proteins extracted from frozen SS samples.

our frozen material prevented us from analyzing whether all these cases were also phosphorylated on serine residues.

The detection of cytoplasmic β-catenin Y142 phosphorylation coupled with a cytoplasmic decoration indicates that this residue may be important for the cytoplasmic localization. This is an intriguing point because, as previously observed in BSS [20], we found that β-catenin expression was restricted to the BSS glandular component, thus indicating a shift from the nucleus to the cytoplasm and/or cytoplasm membrane. In this light, the detection of β-catenin phosphorylation on a Tyr 142 residue in two of our BSS supports the possibility that the change in the localization of β-catenin occurs during the mesenchymal–epithelial transition, particularly because there was no correlation between the transcript type and the type of residue activation.

A clinical trial of geftinib (an EGFR inhibitor) in SS patients with locally advanced or metastatic disease has been conducted in Europe [21], despite the rare occurrence of EGFR mutations [18] and the gain in gene copy number (confirmed by our results). Inhibiting a downstream effector (such as Akt) to block multiple upstream activated RTKs (EGFR, PDGFRα, and PDGFRβ) seems to be a further promising therapeutic possibility as we found that more than one receptor is activated at the same time and direct Akt inhibitors have recently been developed.

It is also worth noting that a previous IHC-based study of non–small cell lung carcinoma [22] found that patients whose surgical specimens showed high levels of both EGFR and Akt activation were more sensitive to RTK inhibitors. Although the results of this study must be considered with caution as the antibody has now been withdrawn from production, the clinical evidence of a response seems to be reliable. We are faced with the problem of the reliability of IHC phospho-specific antibodies every day and find that they do not assure reproducible results, which is why they were not used in the present study.

Our comprehensive investigation of a small, single-center series of SS in children and adolescents adds molecular details to the scanty published findings concerning the biology of pediatric SS. They may also be of interest to clinicians as it is still debated whether SS has the same clinical behavior (and the same biology) in different age groups [23]. This is important because SS are not always treated using the same strategy in different ages, and there is still disagreement between pediatric and adult medical oncologists concerning the role of chemotherapy.

In conclusion, although very preliminary and needing confirmation in a larger series, our finding that multireceptor-mediated Akt activation (and its inhibition by a PI3K inhibitor in the CME-1 SS cell line) may stabilize β-catenin in SS strongly suggests that inhibiting the PI3K/Akt pathway may be a useful adjunctive therapeutic strategy.

References

[1] Allander SV, Illei PB, Chen Y, Antonescu CR, Bittner M, Ladanyi M, and Meltzer PS (2002). Expression profiling of synovial sarcoma by cDNA microarrays: association of ERBB2, IGFBP2, and ELF3 with epithelial differentiation. *Am J Pathol* **161**, 1587–1595.

[2] Thomas DG, Giordano TJ, Sanders D, Biermann S, Sondak VK, Trent JC, Yu D, Pollock RE, and Baker L (2005). Expression of receptor tyrosine kinases epidermal growth factor receptor and HER-2/*neu* in synovial sarcoma. *Cancer* **103**, 830–838.

[3] He XC, Yin T, Grindley JC, Tian Q, Sato T, Tao WA, Dirisina R, Porter-Westpfahl KS, Hembree M, Johnson T, et al. (2007). PTEN-deficient intestinal stem cells initiate intestinal polyposis. *Nat Genet* **39**, 189–198.

[4] Pretto D, Barca R, Rivera J, Neel N, Gustavson MD, and Eid JE (2006). The synovial sarcoma translocation protein SYT–SSX2 recruits β-catenin to the nucleus and associates with it in an active complexes. *Oncogene* **25**, 3661–3669.

[5] Saito T, Oda Y, Sugimachi K, Kawaguchi K, Tamiya S, Tanaka K, Matsuda S, Sakamoto A, Iwamoto Y, and Tsuneyoshi M (2001). E-cadherin gene mutations frequently occur in synovial sarcoma as a determinant of histological features. *Am J Pathol* **159**, 2117–2124.

[6] Saito T, Oda Y, Sakamoto A, Kawaguchi K, Tanaka K, Matsuda S, Tamiya S, Iwamoto Y, and Tsuneyoshi M (2002). APC mutations in synovial sarcoma. *J Pathol* **196**, 445–449.

[7] Nakamura Y (1997). Cleaning up on β-catenin. *Nat Genet* **3**, 499–500.

[8] Tamborini E, Casieri P, Miselli F, Orsenigo M, Negri T, Piacenza C, Stacchiotti S, Gronchi A, Pastorino U, Pierotti MA, et al. (2007). Analysis of potential receptor tyrosine kinase targets in intimal and mural sarcomas. *J Pathol* **212**, 227–235.

[9] Perrone F, Suardi S, Pastore E, Casieri P, Orsenigo M, Caramuta S, Dagrada G, Losa M, Licitra L, Bossi P, et al. (2006). Molecular and cytogenetic subgroups of oropharyngeal squamous cell carcinoma. *Clin Cancer Res* **12**, 6643–6651.

[10] Mancuso T, Mezzelani A, Riva C, Fabbri A, Dal Bo L, Sampietro G, Perego P, Casali P, Zunino F, Sozzi G, et al. (2000). Analysis of *SYT–SSX* fusion transcripts and bcl-2 expression and phosphorylation status in synovial sarcoma. *Lab Invest* **80**, 805–813.

[11] Tamborini E, Papini D, Mezzelani A, Riva C, Azzarelli A, Sozzi G, Pierotti MA, and Pilotti S (2001). c-KIT and c-KIT ligand (SCF) in synovial sarcoma (SS): an mRNA expression analysis in 23 cases. *Br J Cancer* **85**, 405–411.

[12] Surace C, Panagopoulos I, Palsson E, Rocchi M, Mandahl N, and Mertens F (2004). A novel FISH assay for *SS18–SSX* fusion type in synovial sarcoma. *Lab Invest* **84**, 1185–1192.

[13] Winer J, Jung CK, Shackel I, and Wiiliams PM (1999). Development and validation of real-time quantitative reverse transcriptase–polymerase chain reaction for monitoring gene expression in cardiac myocytes *in vitro*. *Anal Biochem* **270**, 41–49.

[14] Signoroni S, Frattini M, Negri T, Pastore E, Tamborini E, Casieri P, Orsenigo M, Da Riva L, Radice P, Sala P, et al. (2007). Cyclooxygenase-2 and platelet-derived growth factor receptors as potential targets in treating aggressive fibromatosis. *Clin Cancer Res* **13**, 5034–5040.

[15] Tamborini E, Bonadiman L, Greco A, Gronchi A, Riva C, Bertulli R, Casali PG, Pierotti MA, and Pilotti S (2004). Expression of ligand-activated KIT and platelet-derived growth factor receptor beta tyrosine kinase receptors in synovial sarcoma. *Clin Cancer Res* **10**, 938–943.

[16] Antonescu CR, Leung DH, Dudas M, Ladanyi M, Brennan M, Woodruff JM, and Cordon-Cardo C (2000). Alterations of cell cycle regulators in localized synovial sarcoma: a multifactorial study with prognostic implications. *Am J Pathol* **156**, 977–983.

[17] Horvai AE, Kramer MJ, and O'Donnell R (2006). β-Catenin nuclear expression correlates with cyclin D1 expression in primary and metastatic synovial sarcoma: a tissue microarray study. *Arch Pathol Lab Med* **130**, 792–798.

[18] Bode B, Frigerio S, Behnke S, Senn B, Odermatt B, Zimmermann DR, and Moch H (2006). Mutations in the tyrosine kinase domain of the EGFR gene are rare in synovial sarcoma. *Mod Pathol* **19**, 541–547.

[19] Lopez-Guerrero JA, Navarro S, Noguera R, Carda C, Farinas SC, Pellin A, and Llombart Bosch A (2005). Mutational analysis of the c-KIT and PDGFRα in a series of molecularly well-characterized synovial sarcomas. *Diagn Mol Pathol* **14**, 134–138.

[20] Saito T, Oda Y, Yamamoto H, Kawaguchi K, Tanaka K, Matsuda S, Iwamoto Y, and Tsuneyoshi M (2006). Nuclear β-catenin correlates with cyclin D1 expression in spindle and pleomorphic sarcomas but not in synovial sarcoma. *Hum Pathol* **37**, 689–697.

[21] Blay JY, Ray-Coquard I, Alberti L, and Ranchère D (2004). Targeting other abnormal signalling pathways in sarcoma: EGFR in synovial sarcoma, PPAR-gamma in liposarcomas. *Cancer Treat Res* **120**, 151–167.

[22] Hirsch FR, Varella-Garcia M, Cappuzzo F, McCoy J, Bemis L, Xavier AC, Dziadziuszko R, Gumerlock P, Chansky K, West H, et al. (2007). Combination of EGFR gene copy number and protein expression predicts outcome for advanced non–small-cell lung cancer patients treated with gefitinib. *Ann Oncol* **4**, 752–760.

[23] Ferrari A, Gronchi A, Casanova M, Meazza C, Gandola L, Collini P, Lozza L, Bertulli R, Olmi P, and Casali PG (2004). Synovial sarcoma: a retrospective analysis of 271 patients of all ages treated at a single institution. *Cancer* **101**, 627–634.